

Adaptive evolution in virulence effectors of the rice blast fungus *Pyricularia oryzae*

Marie Le Naour--Vernet^{1*}, Florian Charriat^{1*}, Jérôme Gracy², Sandrine Cros-Arteil¹, Sébastien Ravel^{1,3}, Florian Veillet¹, Isabelle Meusnier¹, André Padilla², Thomas Kroj¹, Stella Cesari^{1**}, Pierre Gladieux^{1**}

¹PHIM Plant Health Institute, Univ Montpellier, INRAE, CIRAD, Institut Agro, IRD, Montpellier, France

²Centre de Biologie Structurale (CBS), Univ Montpellier, INSERM, CNRS, 29 rue de Navacelles, 34090 Montpellier, France.

³CIRAD, UMR PHIM, 34090 Montpellier, France

* These authors contributed equally to this work

** Corresponding authors:

Pierre Gladieux

Tel: +33 4 99 62 48 17

Email: pierre.gladieux@inrae.fr

Stella Cesari

Tel: +33 4 99 62 48 62

Email: stella.cesari@inrae.fr

Short title: MAX effector evolution in the rice blast fungus

26 ABSTRACT

27 Plant pathogens secrete proteins called effectors that target host cellular processes to promote
 28 disease. Recently, structural genomics has identified several families of fungal effectors that
 29 share a similar three-dimensional structure despite remarkably variable amino-acid sequences
 30 and surface properties. To explore the selective forces that underlie the sequence variability of
 31 structurally-analogous effectors, we focused on MAX effectors, a structural family of effectors
 32 that are major determinants of virulence in the rice blast fungus *Pyricularia oryzae*. Using
 33 structure-informed gene annotation, we identified 58 to 78 MAX effector genes per genome in a
 34 set of 120 isolates representing seven host-associated lineages. The expression of MAX effector
 35 genes was primarily restricted to the early biotrophic phase of infection and strongly influenced
 36 by the host plant. Pangenome analyses of MAX effectors demonstrated extensive
 37 presence/absence polymorphism and identified gene loss events possibly involved in host range
 38 adaptation. However, gene knock-in experiments did not reveal a strong effect on virulence
 39 phenotypes suggesting that other evolutionary mechanisms are the main drivers of MAX effector
 40 losses. MAX effectors displayed high levels of standing variation and high rates of non-
 41 synonymous substitutions, pointing to widespread positive selection shaping the molecular
 42 diversity of MAX effectors. The combination of these analyses with structural data revealed that
 43 positive selection acts mostly on residues located in particular structural elements and at
 44 specific positions. Our work provides unique insights into the evolutionary history of an
 45 extended fungal effector family and opens up new research avenues to deepen our
 46 understanding of the molecular coevolutionary interactions of fungi with plant hosts.

47

48

49 AUTHOR SUMMARY

50 Fungal plant pathogens use small secreted proteins, called effectors, to manipulate to their own
 51 advantage their host's physiology and immunity. The evolution of these effectors, whether
 52 spontaneously or in response to human actions, can lead to epidemics or the emergence of new
 53 diseases. It is therefore crucial to understand the mechanisms underlying this evolution. In this
 54 article, we report on the evolution of effectors in one of the prime experimental model systems
 55 of plant pathology, the fungus causing blast diseases in rice, wheat, and other cereals or grasses.
 56 We identify a particular class of effectors, the MAX effectors, using structural models based on
 57 experimental protein structures of effectors previously shown to have a major role in fungal
 58 virulence. We show that this class of effector is produced by the pathogen during the early stages
 59 of infection, when plant cells are still alive. By comparing the gene content of isolates infecting
 60 different plant species, we show that the MAX effector arsenal is highly variable from one isolate
 61 to another. Finally, using the inferential framework of population genetics, we demonstrate that
 62 MAX effectors exhibit very high genetic variability and that this results from the action of natural
 63 selection.

64

65

66

67

68 INTRODUCTION

69 Plant pathogens secrete effector proteins to manipulate the physiology and metabolism of their
70 host and to suppress its immunity. Consequently, effectors are expected to engage in
71 coevolutionary interactions with plant defense molecules. The proximate mechanisms of
72 effector-driven adaptation are relatively well-characterized: plant pathogens adapt to new hosts
73 through changes in effector repertoires and effector sequences [1, 2]. However, the ultimate
74 (eco-evolutionary) mechanisms underlying effector diversification have remained elusive. The
75 concept of coevolution posits that adaptation in one partner drives counter-adaptations in the
76 coevolving partner [3-5]. Under the co-evolutionary arms race model, variation for disease
77 resistance and pathogen virulence is transient, resulting in a turnover of sequence variation
78 through repeated episodes of strong directional selection [6]. In agricultural systems, because
79 pathogens tend to be ahead of their hosts in the arms race owing to their larger populations and
80 shorter generation times, the co-evolutionary arms race tends to result in so-called boom and
81 bust cycles [7]. Under the alternative, ‘trench warfare’ hypothesis, advances and retreats of
82 resistance or virulence genes frequencies maintain variation as dynamic polymorphisms [8, 9].
83 The maintenance of genetic polymorphisms is called ‘balancing selection’, a process by which
84 different alleles or haplotypes are favored in different places (via population subdivision)
85 and/or different times (via frequency-dependent negative selection). While there is a growing
86 body of data demonstrating the nature and prevalence of the selective pressures that shape the
87 diversity of immune systems in plants [6, 10-12], we still lack a clear picture of the co-
88 evolutionary mechanisms underlying the molecular evolution of virulence factors in their
89 interacting antagonists [13].

90 Effectors from plant pathogenic fungi are typically cysteine-rich secreted proteins
91 smaller than 200 amino acids with an infection-specific expression pattern. Effectors are
92 numerous in fungal genomes (several hundred to more than a thousand per genome), and rarely
93 show homologies with known proteins or domains. They are also highly variable in sequence
94 and do not form large families of sequence homologs. Based on similarity analyses, fungal

95 effectors can form small groups of paralogs (typically with less than five members), but they are
 96 most often singletons. This apparent lack of larger effector families has hindered attempts to
 97 probe into the evolutionary factors underlying their diversification. In addition, the high
 98 diversity of fungal effectors has hampered functional analyses due to the lack of good criteria for
 99 prioritizing them and our inability to predict their physiological role. Consequently, the
 100 virulence function and evolutionary history of most fungal effectors remain unknown.

101 Recently, the resolution of the three-dimensional (3D) structure of fungal effectors
 102 combined with Hidden Markov Model (HMM) pattern searches and structure modeling revealed
 103 that fungal effector repertoires are, despite their hyper-variability, dominated by a limited
 104 number of families gathering highly sequence-diverse proteins with shared structures and,
 105 presumably, common ancestry [14-17]. One such structurally-conserved but sequence-diverse
 106 fungal effector family is the MAX (*Magnaporthe* AvrS and ToxB-like) effector family. MAX
 107 effectors are specific to ascomycete fungi and show massive expansion in *Pyricularia oryzae*
 108 (synonym: *Magnaporthe oryzae*) [17], the fungus causing rice blast disease, one of the most
 109 damaging diseases of rice [18, 19]. MAX effectors are characterized by a conserved structure
 110 composed of six β -strands organized into two antiparallel β -sheets that are stabilized in most
 111 cases by one or two disulfide bridges. The amino acid sequence of MAX effectors is very diverse
 112 and they generally have less than 15% identity, which makes them a family of analogous, not
 113 homologous effectors. MAX effectors are massively expressed during the biotrophic phase of
 114 infection, suggesting an important role in disease development and fungal virulence [17].
 115 Remarkably, about 50% of the known avirulence (AVR) effectors of *P. oryzae* belong to the MAX
 116 family, indicating that these effectors are closely monitored by the host plant immune system
 117 [17].

118 *Pyricularia oryzae* is a multi-host, poly-specialist pathogen that infects more than 50
 119 monocotyledonous plants, including major cereal crops such as rice, maize, wheat, or barley [20-
 120 23]. *Pyricularia oryzae* has repeatedly emerged on new hosts [21, 24], in new geographical areas
 121 [25, 26], and phylogenomic analyses have revealed that it can be subdivided into several genetic

122 lineages, each preferentially associated with a specific or restricted set of host plant genera [27].
 123 In *P. oryzae*, effectors can play a major role in host-shifts or host-range expansions [28-30]. For
 124 example, loss of function of the PWT3 effector in *Lolium*-infecting strains contributed to gain of
 125 virulence on wheat [29]. Similarly, loss of the MAX effector AVR1-CO39 is thought to have
 126 contributed to the emergence of rice blast from foxtail-millet infecting isolates [20, 31]. This
 127 indicates that MAX effectors may be important determinants of host specificity in *P. oryzae*.

128 In this study, we characterized the genetic diversity of MAX effectors in *P. oryzae* and
 129 within its different host-specific lineages. We explored the evolutionary drivers of the
 130 diversification of MAX effectors and tested whether MAX effectors represent important
 131 determinants of *P. oryzae* host specificity. To this aim, we assembled and annotated 120 high-
 132 quality *P. oryzae* genomes from isolates representing seven main host-specific lineages. We
 133 mined these genomes for putative effectors and used hidden Markov models based on fold-
 134 informed protein alignments to annotate putative MAX effectors. We identified 58 to 78 putative
 135 MAX effector genes per individual genome distributed in 80 different groups of MAX homologs.
 136 We showed that the expression of MAX effector genes is largely restricted to the early biotrophic
 137 phase of infection and strongly influenced by the host plant. Our evolutionary analyses showed
 138 that MAX effectors harbor more standing genetic variation than other secreted proteins and
 139 non-effector genes, and high rates of non-synonymous substitutions, pointing to positive
 140 selection as a potent evolutionary force shaping their sequence diversity. Pangenome analyses of
 141 MAX effectors demonstrated extensive presence/absence polymorphism and identified several
 142 candidate gene loss events possibly involved in host range adaptation. Our work demonstrates
 143 that MAX effectors represent a highly dynamic compartment of the genome of *P. oryzae*, likely
 144 reflecting intense co-evolutionary interactions with host molecules.

145 RESULTS

146 *Genome assembly and prediction of MAX effector genes.*

147 We assembled the genomes of a worldwide collection of 120 haploid isolates of *Pyricularia*
148 *oryzae* fungi from 14 host genera: *Oryza* (n=52), *Triticum* (n=21), *Lolium* (n=12), *Setaria*
149 (n=8), *Eleusine* (n=8), *Echinochloa* (n=4), *Zea* (n=4), *Bromus* (n=2), *Brachiaria* (n=2),
150 *Festuca* (n=2), *Stenotaphrum* (n=2), *Eragrostis* (n=1), *Hordeum* (n=1), and *Avena* (n=1) (S1
151 Table). Assembly size ranged from 37Mb to 43.2Mb, with an average size of 40.2 Mb (standard
152 deviation [s.d.]: 1.9Mb). L50 ranged from five to 411 contigs (mean: 97.1; s.d.: 83.2) and N50
153 from 28Kb to 4.0Mb (mean: 238.6Kb; s.d.: 43.8Kb; S1 Table). Gene prediction based on protein
154 sequences from reference 70-15 and RNAseq data identified 11,520 to 12,055 genes per isolate
155 (mean: 11,763.2; s.d.: 103.7). The completeness of assemblies, as estimated using BUSCO [32],
156 ranged between 93.4 and 97.0% (mean: 96.4%; s.d.: 0.6%; S1 Table).

157 MAX effectors were identified among predicted secreted proteins using a combination of
158 similarity searches [33, 34] and structure-guided alignments [35] as summarized in Figure 1. To
159 assess variation in the MAX effector content of *P. oryzae*, we constructed groups of homologous
160 genes (i.e., “orthogroups” or OG) using the clustering algorithm implemented in ORTHOFINDER
161 [36]. A given orthogroup was classified as secreted proteins or MAX effectors if 10% of
162 sequences in the group were identified as such by functional annotation. Sequences were
163 grouped in 14,767 orthogroups, of which 80 were classified as encoding MAX effectors, and
164 3,283 as encoding other types of secreted proteins (Figure 1). The number of MAX orthogroups
165 per isolate ranged from 58 to 73 (average: 65.8; s.d.: 2.8), representing between 58 to 78 MAX
166 genes per isolate (average: 68.4; s.d.: 3.6). The 80 orthogroups of MAX effectors were further
167 split into 94 groups of orthologs, by identifying paralogs using gene genealogies inferred with
168 RAxML v8 [37] (S2 Table).

169

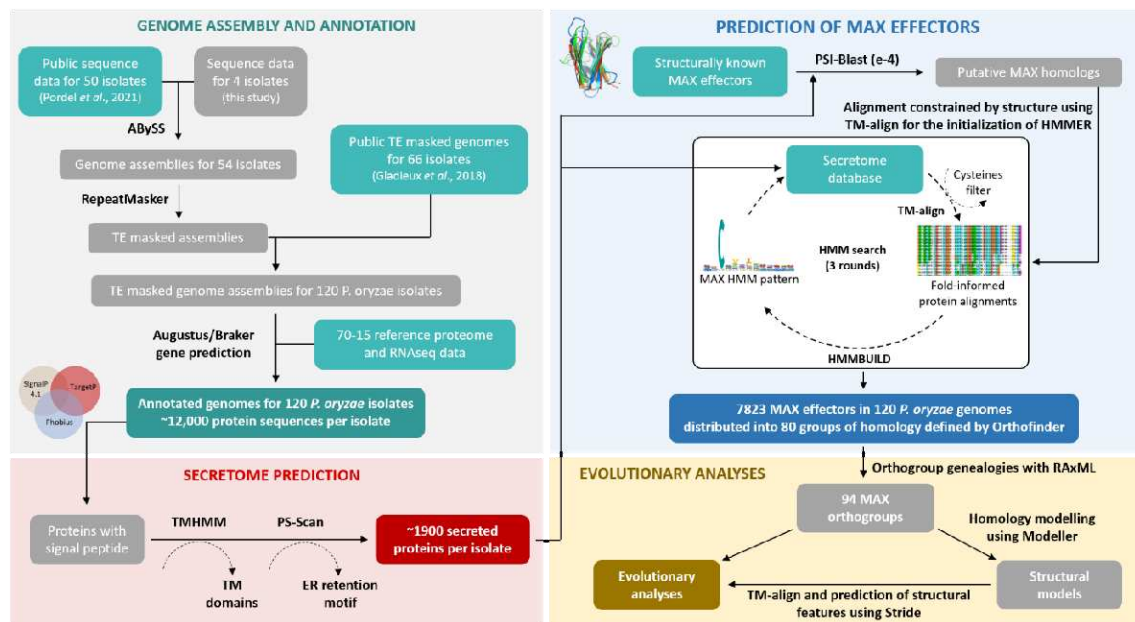


Figure 1. Schematic representation of the key steps of the bioinformatic pipeline used to predict genes in 120 genomes of *Pyricularia oryzae*, and to identify genes encoding MAX effectors. References: Gladieux et al. 2018 [27]; Pordel et al. 2021 [21].

Expression of MAX effector genes during rice infection.

To determine whether these putative MAX effectors are deployed by *P. oryzae* during plant infection, we analyzed the expression patterns of the 67 MAX genes predicted in the genome of the reference isolate Guy11 by qRT-PCR (Figure 2A). Using RNA samples from Guy11 mycelium grown on artificial media, we found that 94% of the MAX genes (63 genes) were not, or very weakly expressed during axenic culture, and only four (i.e., MAX24, MAX29, MAX59, and MAX66) showed weak, medium or strong constitutive expression (Figure 2A). MAX genes were, therefore, predominantly repressed in the mycelium of *P. oryzae*.

Following spray inoculation of Guy11 on the rice cultivar Maratelli, which is highly susceptible to *P. oryzae*, 67% of the MAX genes (45 genes) were expressed (Figure 2A). Among them, three were also expressed in the mycelium (i.e., MAX31, MAX59, and MAX94). MAX31 was over-expressed under infection conditions, whereas the other two showed similar levels of expression *in vitro* and during infection. 64% of the MAX genes (42 genes) showed an infection-specific expression profile with relative expression levels ranging from very low (0.008-0.04) to

very high (>5). Like the *Bas3* gene, encoding a *P. oryzae* effector specifically induced during the biotrophic phase of infection, all *MAX* genes showed maximal expression between the second and fourth day post-inoculation (Figure 2A; S1 Figure).

To test whether the genotype of the host plant could influence the expression of *MAX* genes, we analyzed their expression patterns upon infection of the rice cultivar Kitaake, which has a higher basal resistance to *P. oryzae* than Maratelli (Figure 2A; Figure 2B). During Kitaake infection, 78% of the *MAX* genes (52 genes) were upregulated compared to the *in vitro* condition, while only 64% (43 genes) were induced upon infection of Maratelli (Figure 2A). Some *MAX* genes not expressed in Maratelli were induced in Kitaake (e.g., *MAX24*, *MAX30*, *MAX32*, *MAX43*, *MAX71*, and *MAX73*) (Figure 2B, S2 Figure). Others were significantly upregulated in Kitaake compared to Maratelli (i.e., *MAX22*, *MAX44*, *MAX55*, *MAX57*, *MAX69*, and *MAX91*). However, a few genes, such as *MAX15*, *MAX37* and *MAX62*, among the most strongly expressed effectors in Maratelli, showed weaker levels of expression in Kitaake. These results show that Guy11 deploys a wider diversity of MAX effectors during the infection of Kitaake compared to that of Maratelli, and that MAX effectors are subject to host-dependent expression polymorphism.

Taken together, our data revealed that during the biotrophic phase of rice infection, *P. oryzae* massively deploys MAX effectors in a plastic manner suggesting that they have an important function in fungal virulence.

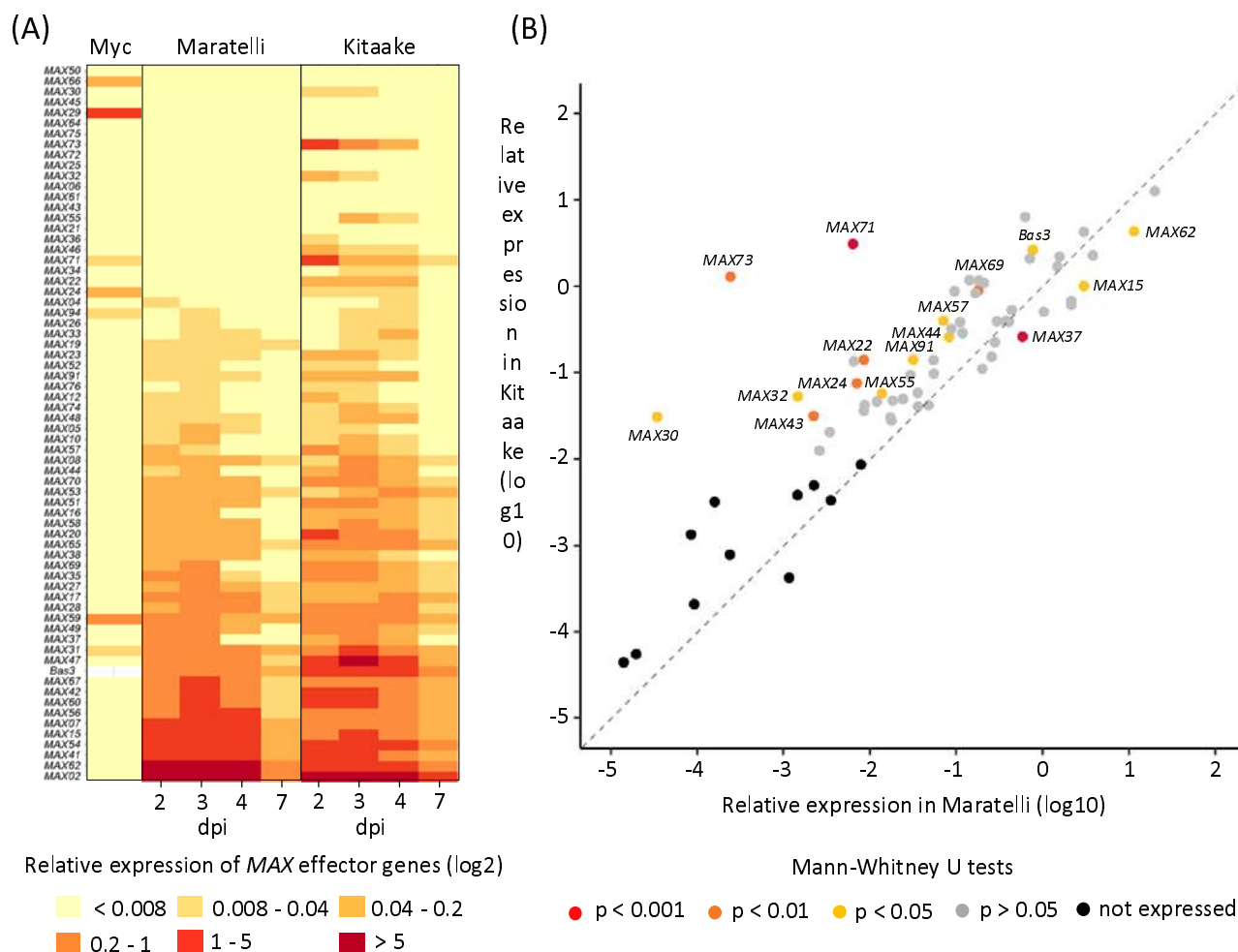


Figure 2. The expression of MAX genes is biotrophy-specific and is influenced by the host plant. (A) Transcript levels of MAX genes and the biotrophy marker gene *Bas3* were determined by qRT-PCR in the mycelium (Myc) of the *P. oryzae* isolate Guy11 grown for 5 days in liquid culture, and in infected leaves of the rice cultivars Maratelli and Kitaake at 2, 3, 4, and 7 days post inoculation (dpi) with Guy11. Relative expression levels were calculated using the constitutively expressed *MoEF1α* (*Elongation Factor 1α*) gene as a reference. The heatmap shows the median relative expression value for each gene (in log2 scale), calculated from 6 independent biological samples for the Myc condition, and 3 independent inoculation experiments (each with 5 independent leaf samples per time point) for each rice cultivar. Effectors were ranked from top to bottom by increasing relative expression values in Maratelli. Relative expression values were assigned to six categories: not expressed (<0.008), very weakly (0.008-0.04), weakly (0.04-0.2), moderately (0.2-1), strongly (1-5) and very strongly expressed (>5). (B) Scatter plot comparing the relative expression levels of MAX genes in Guy11-infected Maratelli and Kitaake cultivars. Each point shows the maximum median relative expression value (in log10 scale) calculated in the infection kinetics described in (A). Difference in effector relative expression levels between the two conditions was assessed by Mann-Whitney U tests and dots were

colored according to significance results: grey ($p > 0.05$), yellow ($p < 0.05$), orange ($p < 0.001$), red ($p < 0.0001$), black (effectors not expressed in both conditions).

Variability of the MAX effector repertoire.

To investigate the genetic diversity of MAX effectors in *P. oryzae*, we analyzed their nucleotide diversity per base pair (π), their ratio of non-synonymous to synonymous nucleotide diversity (π_N/π_S), and their presence-absence polymorphism. Compared to other secreted proteins or other genes, MAX effector orthogroups had higher π , and π_N/π_S values, and lower presence frequency (S3 Figure). Orthogroups including known avirulence genes like *AVR1-CO39*, *AvrPiz-t* and *AVR-Pik* featured among the most diverse orthogroups of MAX effectors (S1 Data).

We categorized genes in the pangenome according to their presence frequencies [38], with core genes present in all isolates, softcore genes present in $>99\%$ isolates, cloud genes present in 1-99% isolates and shell genes present in $<1\%$ isolates. The majority of MAX effector genes were classified as cloud (64/80 [80%] orthogroups), while the majority of other secreted proteins or other genes were classified as core or softcore (1650/3283 [50.2%] and 6714/11404 [58.9%] orthogroups, respectively) (Figure 3A). Only a minority of genes were present in multiple copies (MAX: 15/80 [18.8%]; other effectors: 746/3283 [22.7%]; other genes: 1439/11404 [12.6%]; Figure 3A). Assessment of the openness of the pan-genome by iteratively subsampling isolates revealed a closed pangenome with a limited number of pan and core genes for MAX effectors, other secreted proteins and the remainder of the gene space (Figure 3B). Nucleotide diversity differed significantly between categories of the pangenome for non-MAX effectors (Kruskal-Wallis test: $H=181.17$, d.f.=2, $p < 0.001$) and other genes (Kruskal-Wallis test: $H=225.25$, d.f.=2, $p < 0.001$), but not for MAX effectors (Kruskal-Wallis test: $H=2.50$, d.f.=2, $p > 0.05$). For non-MAX effectors and other genes, nucleotide diversity π was significantly higher in the cloud genes than in softcore genes and core genes (Post-hoc Mann-Whitney U-tests, $p < 0.001$; Figure 3C).

Together, these analyses show that the MAX effector repertoire is highly plastic compared to other gene categories, both in terms of the presence/absence of orthogroups and the sequence variability within orthogroups.

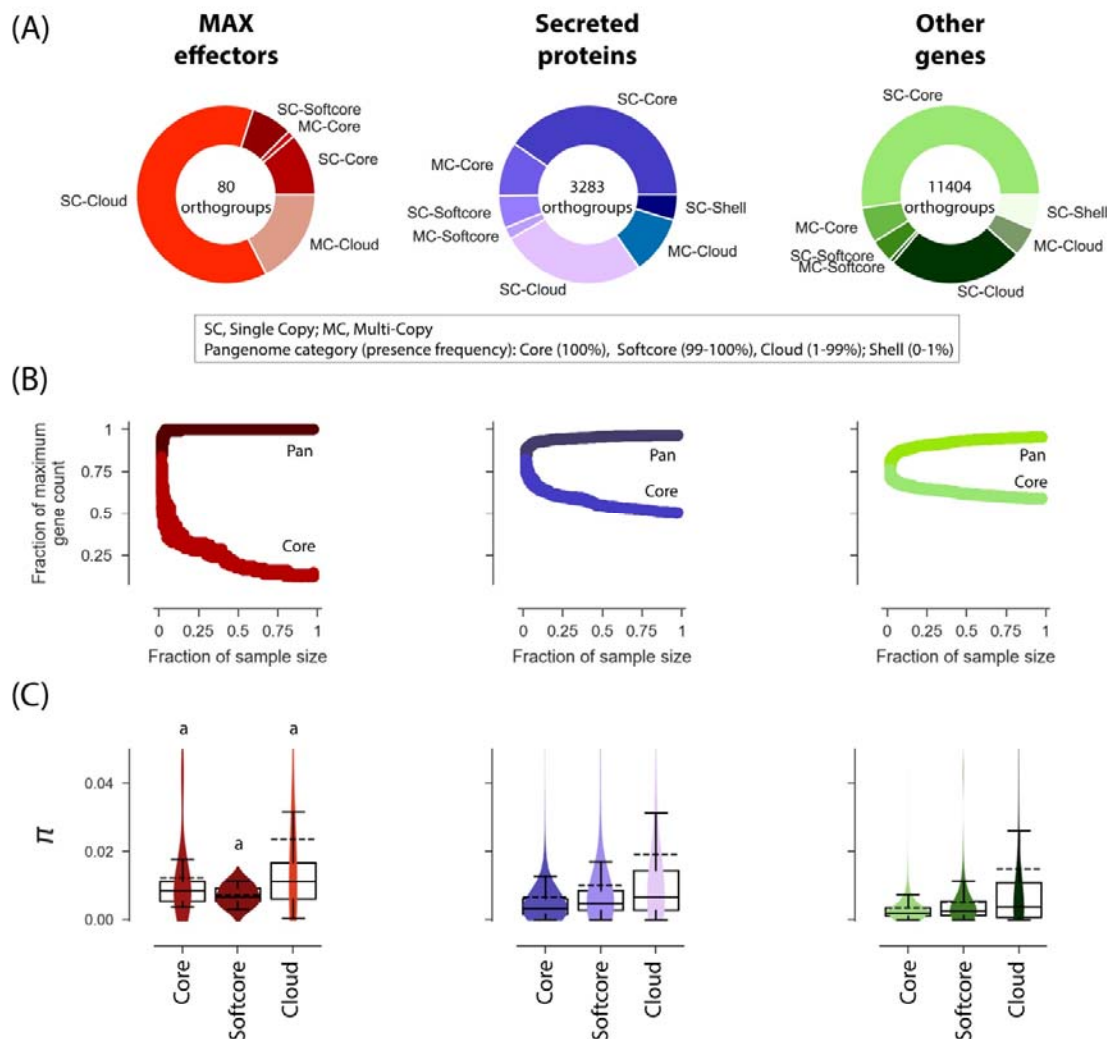


Figure 3. The pan-genome of *P. oryzae*. (A) Composition of the pan-genome of MAX effectors, other secreted proteins, and other genes. (B) Rarefaction analysis of the size of pan- and core-genomes. For k ranging from two to the sample size minus one, pan- and core-genome sizes were computed for 1000 random combinations of k isolates. Subsample size is represented as a fraction of the sample size ($n=121$), and pan- and core-genome sizes as a fraction of maximum gene counts (reported at the center of donut plots in panel A). “core” genes are present in all isolates of a pseudo-sample of size k ; “pan” qualifies genes that are not “core”. (C) Nucleotide diversity per base pair (π) in core, softcore, and cloud genes. A number of data points were cropped from the nucleotide diversity plot for visually optimal presentation but included in statistical tests. In box plots, the dashed black line is the mean, the solid black line is the

264 median. Shell genes were not included in the nucleotide diversity plot because it was not computable due to the small
265 sample size or lack of sequence after filtering for missing data. Shared superscripts indicate non-significant
266 differences (Post-hoc Mann-Whitney U-tests).
267

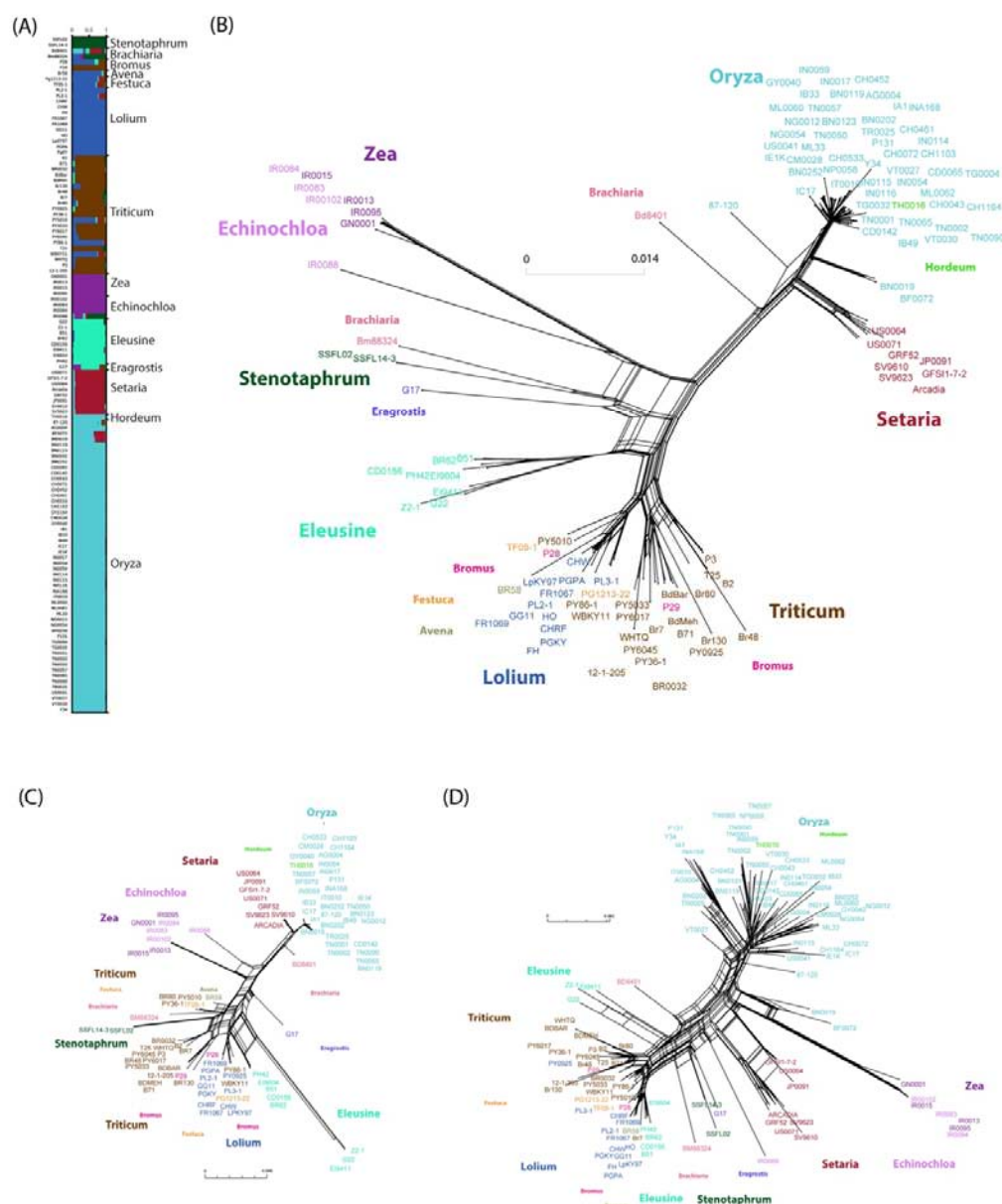
268 *Population subdivision.*

269 To investigate signatures of positive selection in the genome of *P. oryzae*, and identify candidate
 270 loci involved in host specificity, we first identified the divergent lineages represented in our
 271 dataset. We inferred population structure from 5.04e5 SNPs in single-copy core orthologs, using
 272 complementary approaches that make no assumption about random mating or linkage
 273 equilibrium. Both clustering analyses with the sNMF software [38] (Figure 4A) and neighbor-net
 274 phylogenetic networks [39] (Figure 4B) revealed consistent patterns that split genetic variation
 275 primarily by host of origin, with seven major lineages mainly associated with rice (*Oryza*),
 276 foxtail millet (*Setaria*), wheat (*Triticum*), ray-grass (*Lolium*), goosegrass (*Eleusine*), barnyard
 277 grass and maize (*Echinochloa* and *Zea*), and St. Augustine grass (*Stenotaphrum*).

278 Population subdivision inferred from MAX effectors using either 130 SNPs without
 279 missing data in single-copy core MAX effectors (Figure 4C) or presence/absence variation of all
 280 80 MAX effector orthogroups (Figure 4D) revealed essentially the same groups as the analysis of
 281 the single-copy core orthologs. This indicates that genome-wide nucleotide variation, variation
 282 in MAX effector content, and nucleotide variation at MAX effectors reflected similar genealogical
 283 processes. The *Oryza* and *Setaria* lineages displayed exceptionally high presence/absence
 284 variation of MAX effectors (average Hamming distance between pairs of isolate: 0.123 and
 285 0.095; Figure 4D), but only limited sequence variation at single copy core MAX effectors
 286 (average Hamming distance between pairs of isolate: 0.017 and 0.012; Mann-Whitney U-tests,
 287 $p < 0.05$; Figure 4C).

288 Population subdivision was also apparent at the level of the global characteristics of
 289 genomes. Assembly size differed significantly among lineages (Kruskal-Wallis test: $H=72.9$,
 290 d.f.=4, $p < 0.0001$), and genome assemblies for the *Oryza*-infecting lineage, in particular, were
 291 significantly shorter than assemblies from other groups (Post-hoc Mann-Whitney U-tests,
 292 $p < 0.001$; S4 Figure). The number of predicted genes, which was positively and significantly
 293 correlated with assembly size (Spearman's $\rho=0.31$, $p < 0.001$), also differed significantly among
 294 lineages and was the highest in the *Lolium*-infecting lineage and the lowest in the *Eleusine*-

295 infecting lineage (Kruskal-Wallis test: $H=19.4$, $d.f.=4$, $p<0.0001$; S4 Figure). The distribution of
 296 the number of orthogroups in lineages was largely similar to the distribution of the number of
 297 genes, with more orthogroups in the *Lolium*-infecting lineage and fewer in the *Eleusine*-infecting
 298 lineage (S4 Figure).



299
 300 Figure 4. Population subdivision in 120 isolates of *Magnaporthe oryzae*. Population subdivision was inferred from (A-
 301 B) 5.04e5 single nucleotide polymorphisms (SNPs) without missing data identified in coding sequences of single-copy
 302 core orthologs, (C) 130 SNPs without missing data identified in coding sequences of single-copy MAX effectors,
 303 (D) a table of presence/absence data (coded as 0 and 1) for all 80 MAX effector orthogroups. (A) Genetic ancestry

proportions for individual isolates in K=7 ancestral populations, as estimated using the sNMF clustering algorithm [38]; each isolate is depicted as a horizontal bar divided into K segments representing the proportion of ancestry in K=7 inferred ancestral populations; host genus of origin is indicated on the right side. (B-D) Neighbor-net phylogenetic networks estimated with SPLITSTREE [39], with isolate names colored according to their host of origin. In (C), haplotypes repeated multiple times were represented by the first items in the following lists: (BN0252, CD0065, CH0043, CH0072, CH0452, CH0461, IN0114, IN0115, IN0116), (IB33, ML0060, ML0062, ML33, NG0054, NP0058, TG0004, TG0032, US0041, VT0027, VT0030), (TR0025, Y34), (CHRF, HO, LPKY97, P28).

Loss of MAX effectors in specific lineages does not necessarily associate with host specificity.

The comparison of the MAX effector content in the genomes of 120 *P. oryzae* isolates revealed extensive presence/absence polymorphism between host-specific groups (S3 Table). To address the underlying evolutionary mechanisms, we tested experimentally the hypothesis that MAX effector losses are massively related to escape from receptor-mediated non-host resistance. Indeed, the loss of MAX effectors in specific lineages of *P. oryzae* could primarily serve to escape from non-host resistance during infections of novel plant species carrying immune receptors specifically recognizing these effectors. To test this hypothesis, we focused on the *Oryza*- and *Setaria*-infecting lineages, as previous investigations suggested that the *Oryza*-infecting lineage emerged by a host shift from *Setaria* and we found both groups to be closely related (Figure 4) [21, 40]. Our strategy was to introduce into the *Oryza*-isolate Guy11 MAX effectors absent from the *Oryza* lineage but present in the *Setaria* lineage, and to assess the ability of these transgenic isolates to infect rice.

We identified three MAX orthogroups that were largely or completely absent from the *Oryza* lineage, but present in the majority of isolates of the other lineages (S3 Table). Orthogroup MAX79 (OG0011591-1) was absent in all 52 *Oryza*-infecting isolates, while MAX83 (OG0011907), and MAX89 (OG0012141) were absent in 50 and 46 of them, respectively (S3 Table). Constructs carrying the genomic sequence of *MAX79*, *MAX83* or *MAX89* derived from the *Setaria* isolate US0071 and under the control of the strong infection specific promoter of the effector *AVR-Pia* were generated and stably introduced into Guy11. For each construct, three independent transgenic lines were selected. Transgene insertion was verified by PCR and the

expression of transgenes was measured by qRT-PCR (S5 Figure). To test whether the selected MAX effectors trigger immunity in rice, the transgenic isolates were spray-inoculated onto a panel of 22 cultivars representative of the worldwide diversity of rice (S4 Table).

As controls, we used the MAX effectors *AVR-Pia*, which is rare outside the *Oryza* and *Setaria* lineages, and *AVR1-CO39*, which is absent or pseudogenized in the *Oryza* lineage, but present in all other host-specific lineages including *Setaria*. Both effectors are detected in rice by the paired NLR immune receptors RGA4 and RGA5 from the *Pi-a/Pi-CO39* locus and thereby contribute, respectively, to host or non-host resistance in this plant species [41, 42].

As expected, isolates expressing *AVR1-CO39* or *AVR-Pia* triggered resistance in the rice variety Aichi Asahi that carries *Pi-a*, but caused disease on Nipponbare (*pi-a*) and other varieties lacking this *R* locus (Figure 5; S4 Table). Unlike the positive controls, the effectors MAX79, MAX83 and MAX89 were not recognized and did not induce resistance in any of the tested rice cultivars (Figure 5; S4 Table). The disease symptoms caused by the transgenic isolates carrying these effectors were similar to those observed for wild-type Guy11 or Guy11 isolates carrying an *RFP* (red fluorescent protein) construct. This suggests that these effectors do not significantly increase the virulence of Guy11.

These experiments show that despite their loss in the *Oryza*-infecting lineage of *P. oryzae*, and unlike *AVR1-CO39*, the effectors MAX79, MAX83, and MAX89 do not seem to induce non-host resistance in rice. Consequently, other mechanisms than escape from host immunity contributed to the loss of these MAX effectors during the putative host shift of *P. oryzae* from *Setaria* to *Oryza*.

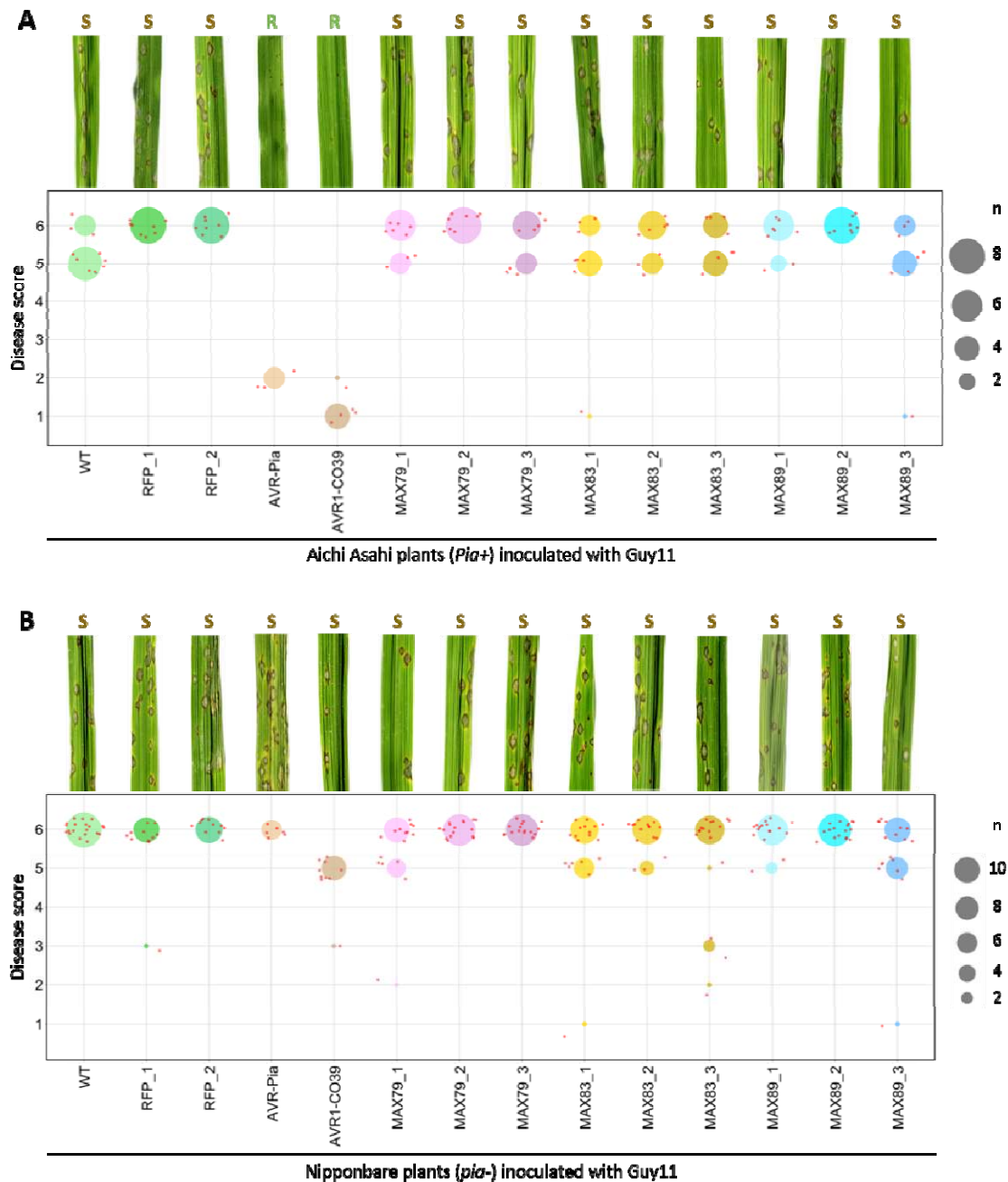


Figure 5. AVR1-CO39 contributes to non-host specificity in rice but not MAX79, MAX83 or MAX89. Wild type and transgenic isolates of *P. oryzae* Guy11 expressing the *RFP* (red fluorescent protein), *AVR-Pia*, *AVR1-CO39*, *MAX79*, *MAX83* or *MAX89* gene were spray-inoculated at 40 000 spores/ml on three-week-old rice plants of the cultivars Aichi Asahi (A) and Nipponbare (B). For each condition, representative disease phenotypes on rice leaves at seven days post-inoculation are shown (top panels, R: resistance, S: susceptibility). Disease phenotypes were also scored (from 1 [complete resistance] to 6 [high susceptibility]) on leaves from 3 to 5 individual rice plants and data are shown as dot plots (bottom panels). The size of each circle is proportional to the number of replicates (n) matching the corresponding score for each condition. Small red dots correspond to individual measurements. The experiment was

performed twice for Aichi Asahi and four times for Nipponbare for all isolates except for WT, AVR-Pia, and AVR1-CO39 control isolates. For these isolates, experiments were performed once on Aichi Asahi and twice on Nipponbare because disease phenotypes are well characterized in the literature.

Signatures of balancing selection at MAX effectors.

To investigate the impact of balancing selection on MAX effector evolution, we focused on single-copy core, softcore, and cloud orthogroups to avoid the possible effect of gene paralogy. We then computed π (nucleotide diversity per bp), F_{ST} (the amount of differentiation among lineages [43]), π_N (non-synonymous nucleotide diversity), π_S (synonymous nucleotide diversity), and π_N/π_S (the ratio of non-synonymous to synonymous nucleotide diversity). Large values of π and π_N/π_S , in particular, are possible indicators of a gene being under balancing selection.

Nucleotide diversity (π) differed significantly between groups of genes (Kruskal-Wallis test, $H=509.9$, $d.f.=2$, $p < 0.001$; Figure 6A; S5 Table). π was significantly higher for the set of MAX effectors (average π : 0.0104, standard deviation: 0.0137), than for other secreted proteins (average π : 0.0079, standard deviation: 0.020), and other genes (average π : 0.0049, standard deviation: 0.014; Mann-Whitney U-tests, $p < 0.05$), showing that MAX effectors, and to a smaller extent other secreted proteins, are more variable than a typical gene. At the lineage level, however, nucleotide diversity at MAX effectors tended to not significantly differ from other putative effectors, or other genes (S5 Table).

In addition to having greater nucleotide variation than other genes at the species level, MAX effectors also displayed a higher ratio of non-synonymous to synonymous nucleotide diversity (Figure 6B; S5 Table). The π_N/π_S ratio differed significantly between groups of genes (Kruskal-Wallis tests $H=101.4$, $d.f.=2$, $p < 0.001$), and the excess of non-synonymous diversity was significantly, and markedly, higher for MAX effectors (average π_N/π_S : 1.826, standard deviation: 3.847) than for other effectors (average π_N/π_S : 0.461, standard deviation: 1.600), and other genes (average π_N/π_S : 0.448, standard deviation: 1.463; Mann-Whitney U-tests, $p < 0.05$). The higher π_N/π_S of MAX effectors was mostly driven by differences in π_N (Figure 6A; S5 Table). Twenty MAX effectors displayed values in the top 5% percentile of non-effector genes, far

exceeding the four genes expected by chance ($p < 0.05$). More specifically, 26 MAX effectors displayed π_N/π_S values greater than 1, which is the value expected under neutrality. This included three well-known avirulence genes: *AVR1-CO39* ($\pi_N/\pi_S = 2.564$), *AVR-Pik* ($\pi_N/\pi_S = 15.574$), and *AvrPiz-t* ($\pi_N/\pi_S = 1.431$). The average π_N/π_S ratio was also higher at MAX effectors than other secreted proteins and other genes in all lineages, with significant differences in four lineages (Mann-Whitney U-tests, $p < 0.05$), and the average π_N/π_S was greater than one in the *Oryza* lineage (Figure 6B; S5 Table). Seven to eleven MAX effectors had $\pi_N/\pi_S > 1$ at the lineage level, representing 8% (*Setaria*-infecting lineage) to 41% (*Lolium*-infecting lineage) of MAX effectors with a defined π_N/π_S ratio (*Zea/Echinochloa* lineage excluded, as only three MAX effectors had a defined π_N/π_S ; S2 Data).

$\pi_N/\pi_S > 1$ is a strong indication of multiallelic balancing selection (*i.e.*, multiple alleles at multiple sites are balanced), as single sites under very strong balancing selection cannot contribute enough non-synonymous variability to push the π_N/π_S ratio above one [44]. To assess whether the adaptation of lineages to their respective hosts may contribute to the species-wide excess of non-synonymous diversity detected at MAX effectors, we estimated population differentiation. The differentiation statistic F_{ST} differed significantly between groups of genes (Kruskal-Wallis tests $H = 8.731$, $d.f. = 2$, $p = 0.013$), and differentiation was significantly higher for MAX effectors than for other secreted proteins and other genes (Figure 6A; S5 Table). F_{ST} was also significantly, albeit relatively weakly, correlated with π_N/π_S at MAX effectors (Spearman's ρ : 0.304, $p = 0.007$; S6 Figure). These observations indicate that between-lineages differences in allele frequencies are greater for MAX effectors than for other secreted proteins or other genes, which may result from divergent selection exerted by hosts.

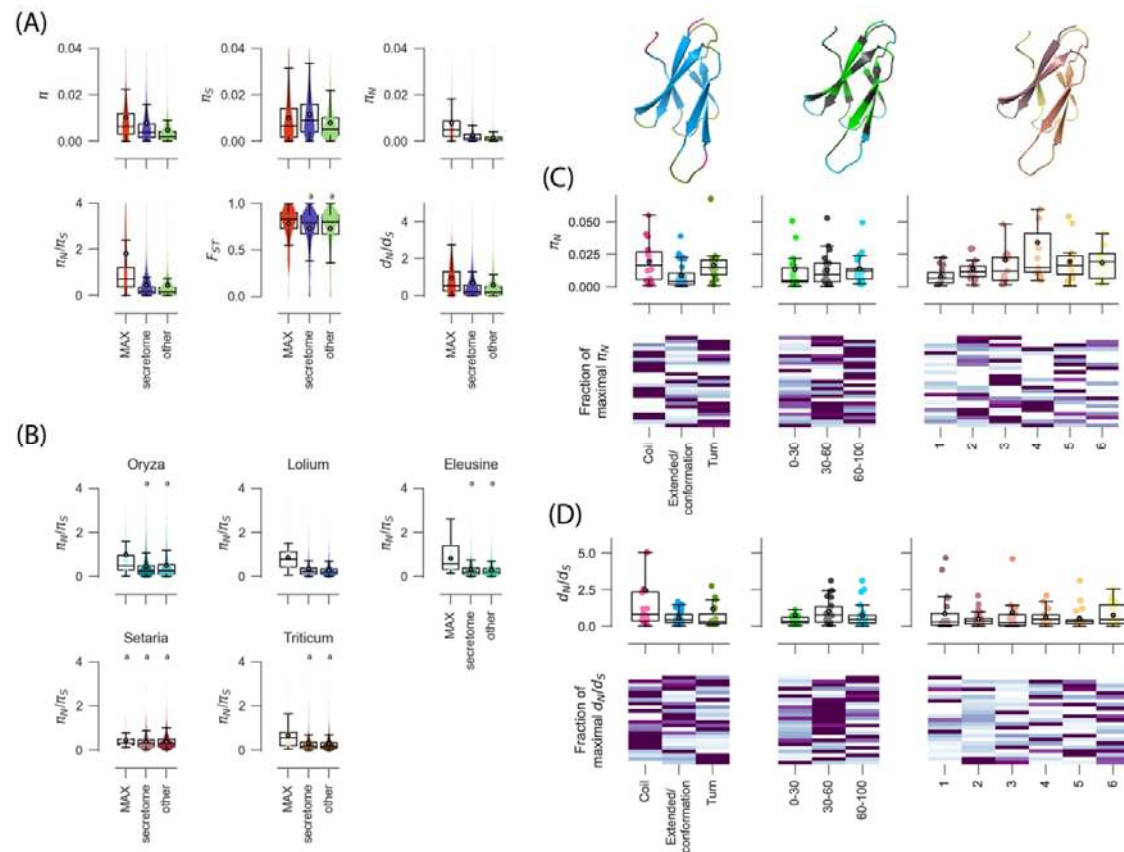


Figure 6. Summary statistics of polymorphism and divergence at MAX effectors, other secreted proteins (i.e., secretome), and other genes of *P. oryzae*. (A) Species-wide estimates of π (nucleotide diversity per bp), F_{ST} (the amount of differentiation among lineages), π_N (non-synonymous nucleotide diversity per bp), π_S (synonymous nucleotide diversity per bp), π_N/π_S (the ratio of non-synonymous to synonymous nucleotide diversity), d_N/d_S (the ratio of non-synonymous to synonymous rates of substitutions). (B) Lineage-specific estimates of π_N/π_S . (C) and (D) Species-wide estimates of π_N and d_N/d_S computed at MAX effectors with signatures of balancing selection ($\pi_N/\pi_S > 1$; panel C) and signatures of directional selection ($d_N/d_S > 1$; panel D) for different classes of secondary structure annotations highlighted on the three-dimensional structure of *AVR-Piz-t* above panel C: (i) structural features, with three subclasses: “extended conformation”, “coils”, and “turns”; (ii) solvent accessibility percentage of the Van der Waals surface of the amino acid sidechain, with three sub-classes: 0-30% (buried), 30-60% (intermediate), and 60-100% (exposed); (iii) structural domains, with six subclasses that grouped the coil, extended conformation and turn residues that define the six beta strands characteristic of MAX effectors. In the heatmaps, each line represents a MAX effector. For a given MAX effector and a given structural feature, the darkest color indicates the class of the secondary structure annotation for which the summary statistic is the highest. Only single-copy core, softcore, and cloud groups of orthologous genes were included in calculations. Shared superscripts indicate non-significant differences (post-hoc Mann-Whitney U-tests, $p > 0.05$). A number of data points were cropped from plots in (A) and (B) for visually optimal presentation but included in statistical tests. In box plots, the black circle is the mean, the black line is the median.

436

437 *Signatures of recurrent directional selection at MAX effectors*

438 To detect adaptive molecular evolution, we collected orthologous sequences from outgroup
 439 *Pyricularia sp.* LS [45, 46] and estimated the d_N/d_S ratio (the ratio of non-synonymous to
 440 synonymous substitution rates) using a maximum likelihood method [47]. Outgroup sequences
 441 could be retrieved for 10,174 out of 14,664 single-copy orthogroups, including 66 out of 94
 442 single-copy orthologs of MAX effectors. The d_N/d_S ratio differed significantly between groups of
 443 genes (Kruskal-Wallis tests $H=45.812$, $d.f.=2$, $p<0.001$; Figure 6A; S5 Table), and was higher for
 444 MAX effectors (average d_N/d_S : 0.977, s.d.: 1.316) than for other secreted proteins (average
 445 d_N/d_S : 0.711, s.d.: 1.722), and other genes (average d_N/d_S : 0.584, s.d.: 1.584; Mann-Whitney U-
 446 tests, $p<0.05$). The same pattern of higher d_N/d_S for MAX effectors was observed at the lineage
 447 level (S5 Table). Twenty-four of the 66 MAX effectors with outgroup sequence (i.e., 36.4%)
 448 showed $d_N/d_S>1$ (S2 Data), which is a strong indication of directional selection. $d_N/d_S>1$ is only
 449 expected for genes that have experienced repeated bouts of directional selection which led to
 450 repeated fixations of amino-acid substitutions [44]. Eleven MAX effectors displayed signatures of
 451 both multiallelic balancing selection ($\pi_N/\pi_S>1$) and multiallelic directional selection ($d_N/d_S>1$).

452 The divergence data, therefore, indicate that a scenario of molecular co-evolution
 453 involving repeated selective sweeps may apply to a substantial fraction (at least one-third) of
 454 MAX effectors.

455

456 *Structural determinants of polymorphism and divergence at MAX effectors.*

457 Different parts of proteins can be under different selective forces. To investigate the
 458 relationships between the structural properties of MAX effectors and signatures of balancing or
 459 directional selection, we focused on MAX effectors with d_N/d_S and π_N/π_S ratios >1 and we
 460 computed π_N and d_N/d_S for different classes of secondary structure annotations, as computed by
 461 STRIDE from MAX effector structures predicted by homology modeling for each orthologous
 462 group [48] (S7 Figure). We used π_N and not π_N/π_S because the latter tended to be undefined due

to relatively short sequence lengths. We defined three classes of secondary structure annotations: (1) structural features, with three subclasses: “extended conformation”, “coils”, and “turns”; (2) solvent accessibility percentage of the Van der Waals surface of the amino acid sidechain, with three sub-classes: 0-30% (buried), 30-60% (intermediate), and 60-100% (exposed); (3) structural domains, with six subclasses that grouped the coil, extended conformation and turn residues that define the six beta strands characteristic of MAX effectors. We used the structure-guided alignment generated by TM-ALIGN to extract the secondary structure annotations of each amino acid of the MAX effector sequences (S7 Figure).

We found that π_N significantly differed (Kruskal-Wallis tests $H=8.504$, $d.f.=2$, $p=0.014$) between subclasses of structural features (Figure 6C; S6 Table). In the 25 MAX effectors under multiallelic balancing selection that passed our filter on sequence length (at least ten sequences longer than 10bp, see Methods), π_N was significantly higher at coils and turns, than at extended conformations (coils: $\pi_N=0.0191$; turns: $\pi_N=0.0167$; extended conformations: $\pi_N=0.0086$; posthoc Mann-Whitney U-tests, $p<0.05$), and 10 and 9 MAX effectors displayed their highest values of π_N in coils and turns, respectively. π_N did not significantly differ between relative solvent accessibility subclasses (Kruskal-Wallis tests $H=2.308$, $d.f.=2$, $p=0.315$), but differences were marginally significant between structural domains (Kruskal-Wallis tests $H=11.035$, $d.f.=5$, $p=0.051$). The third, fourth and fifth beta strands displayed the highest levels of non-synonymous diversity ($\pi_N=0.0341$, $\pi_N=0.0341$, and $\pi_N=0.0341$, respectively), and 18 out of 25 MAX effectors displayed their highest values of π_N at one of these three beta strands (S6 Table).

In the 23 MAX effectors under multiallelic directional selection that passed our filter on sequence length (at least ten sequences longer than 10bp, see Methods), differences in d_N/d_S were most pronounced between subclasses of structural features (Kruskal-Wallis tests $H=5.499$, $d.f.=2$, $p=0.064$), with higher average d_N/d_S values for coils and turns ($d_N/d_S=2.490$ and $d_N/d_S=1.184$, respectively) than extended conformations ($d_N/d_S=0.573$) (Figure 6D; S6 Table). The average d_N/d_S was also close to one for the 30-60% subclass of relative solvent

accessibility ($d_N/d_S=0.994$), and 12 MAX effectors with signatures of directional selection had their highest d_N/d_S values for this subclass, although differences were not significant.

Overall, these analyses show that multiallelic balancing and directional selection acted preferentially on coils and turns, but that the impact of two forms of selection on structural domains and solvent accessibility subclasses differs.

DISCUSSION

MAX effectors as model systems to investigate effector evolution.

Effectors involved in coevolutionary interactions with host-derived molecules are expected to undergo non-neutral evolution. Yet, the role of natural selection in shaping polymorphism and divergence at effectors has remained largely elusive [2]. Despite the prediction of large and molecularly diversified repertoires of effector genes in many fungal genomes, attempts to probe into the evolutionary drivers of effector diversification in plant pathogenic fungi have been hindered by the fact that, until recently, no large effector families had been identified. In this study, we overcome the methodological and conceptual barrier imposed by effector hyperdiversity by building on our previous discovery [17] of an important, structurally-similar, but sequence-diverse family of fungal effectors called MAX. We used a combination of structural modeling, evolutionary analyses, and molecular plant pathology experiments to provide a comprehensive overview of polymorphism, divergence, gene expression, and presence/absence at MAX effectors. When analyzed species-wide or at the level of sub-specific lineages, ratios of non-synonymous to synonymous nucleotide diversity, as well as ratios of non-synonymous to synonymous substitutions, were consistently higher at MAX effectors than at other loci. At the species level, the two ratios were also significantly higher than expected under the standard neutral model for a large fraction of MAX effectors. The signatures of adaptive evolution detected at MAX effectors, combined with their extensive presence/absence variation, are

consistent with their central role in coevolutionary interactions with host-derived ligands that impose strong selection on virulence effectors.

Adaptive evolution at MAX effectors

Rates of evolution determined from orthologous comparisons with outgroup sequences revealed that, for a large fraction of MAX effectors, non-synonymous changes have accumulated faster than synonymous changes. The fast rate of amino-acid change at MAX effectors is consistent with a classic arms race scenario, which entails a series of selective sweeps as new virulent haplotypes - capable of avoiding recognition by plant immune receptors that previously prevented pathogen multiplication - spread to high frequency [49, 50]. Furthermore, it is important to note that although large values of the d_N/d_S ratio provide strong evidence for directional selection, small values do not necessarily indicate the lack thereof, as d_N/d_S ratios represent the integration of genetic drift, constraint, and adaptive evolution [50][51]. Much of the adaptive changes at MAX effectors probably took place before the radiation of *P. oryzae* on its various hosts. However, the observation that d_N/d_S values determined from orthologous comparisons with outgroup are higher at the species level than at the sub-specific lineage level indicates that part of the signal of directional selection derives from inter-lineage amino acid differences associated with host-specialization. Our structural modeling indicates that it is preferentially “turns” and “coils”, but also residues with intermediate solvent accessibility, which often evolve at an unusually fast rate, and therefore that these are probably the residues of MAX proteins preferentially involved in coevolutionary interactions with host-derived molecules.

MAX effectors are characterized by a remarkable excess of non-synonymous polymorphism, compared to synonymous polymorphism, at the species level, but also - albeit to a lesser extent - at the sub-specific lineage level. This raises the question of how polymorphisms are maintained in the face of adaptive evolution, given that selective sweeps under a classic arms race scenario are expected to erase variation [6, 9]. Directional selection restricted to host-

specific lineages - i.e., local adaptation - may contribute to the signature of multiallelic balancing selection observed at the species level. The observation of a positive correlation between π_N/π_S and the differentiation statistic F_{ST} , together with the fact that most MAX effectors are monomorphic at the lineage level, are consistent with a role of divergent selection exerted by hosts in the maintenance of species-wide diversity at MAX effectors. However, the finding that MAX effectors with a defined π_N/π_S at the sub-specific lineage level (i.e., MAX effectors with $\pi_S \neq 0$) present a higher ratio than the other genes also indicates that the adaptive evolution process is not simply one of successive selective sweeps. This is consistent with balancing selection acting at the lineage level, through which polymorphisms in MAX virulence effectors are maintained due to spatiotemporal variation in selection pressures posed by the hosts – a process known as the trench-warfare model [49]. Our structural modeling suggests in particular that the “coils” and “turns” are the preferred substrate of these coevolutionary interactions leading to the maintenance of elevated polymorphism at MAX virulence effectors.

Expression kinetics of MAX effectors

Expression profiling showed that the MAX effector repertoire was induced specifically and massively during infection. Depending on the host genotype, between 64 and 78% of the MAX effectors were expressed and expression was particularly strong during the early stages of infection. These findings are consistent with previous studies that analyzed genome-wide gene expression during rice infection or specifically addressed MAX effector expression, and they reinforce the hypothesis that MAX effectors are crucial for fungal virulence and specifically involved in the biotrophic phase of infection [17, 52].

How this coordinated deployment of the MAX effectors is regulated remains largely unknown. Genome organization does not seem to be a major factor, since MAX effectors do not colocalize and more generally, there is no clustering of effectors in the *P. oryzae* genome, only a slight enrichment in subtelomeric regions [52, 53]. This differs from other pathogenic fungi,

such as *Leptosphaeria maculans*, for which early-expressed effectors are clustered in AT-rich isochores, and co-regulated by epigenetic mechanisms [54]. Analysis of promoter regions of MAX effectors did not identify common DNA motifs that may be targeted by transcription factors, and no such transcriptional regulators that would directly regulate large fractions of the effector complement of *P. oryzae* have been identified yet. The few known transcriptional networks controlled by regulators of *P. oryzae* pathogenicity generally comprise different classes of fungal virulence genes such as secondary metabolism genes or carbohydrate-active enzymes; they are not restricted to effectors or enriched in MAX effectors. For instance, Rgs1, a regulator of G-protein signaling necessary for appressorium development, represses the expression of 60 temporally co-regulated effectors in axenic culture and during the pre-penetration stage of plant infection [55]. However, among them are only two MAX effectors, *MAX15* (*MGG05424*) and *MAX67* (*MGG16175*). This suggests that multiple complementary mechanisms contribute to the precise coordination of MAX effector expression during rice invasion.

Expression profiling also revealed that the plant host genotype strongly influenced the expression of the MAX effector repertoire, suggesting that plasticity in effector expression may contribute to the adaptation of *P. oryzae* to its hosts. MAX effectors were stronger expressed in the more resistant Kitaake rice variety than in highly susceptible Maratelli rice. This is reminiscent of other pathogenic fungi, such as *Fusarium graminearum* and *L. maculans*, for which a relationship between host resistance levels and effector expression was established [56, 57]. Specific experiments will have to be performed to analyze in more detail this potential link between plant resistance and MAX effector expression.

Presence/absence polymorphism of MAX effectors

Pangenome analyses demonstrated extensive variability in the MAX effector repertoire. In cases where MAX effectors are specifically absent from some lineages, but present in most or all others, it is tempting to hypothesize that they experienced immune-escape loss-of-function

mutations that directly contributed to host range expansion or host shifts. A possible example of such a mechanism is the non-MAX effector *PWT3* of *P. oryzae* that is specifically absent from the *Triticum*-infecting lineage [29]. *PWT3* triggers resistance in wheat cultivars possessing the *RWT3* resistance gene [58], and its loss was shown to coincide with the widespread deployment of *RWT3* wheat. Similarly, the loss of the effector *AVR1-CO39* (*MAX86*), which is specifically absent from the *Oryza*-infecting lineage and that is detected by the rice NLR immune receptor complex RGA4/RGA5, has been suggested to have contributed to the initial colonization of rice by the *Setaria*-infecting lineage [20, 31, 59]. Two other orthologous *P. oryzae* effectors, *PWL1* and *PWL2*, exclude Eleusine and rice-associated isolates from infecting *Eragrostis curvula*, and can, therefore, also be considered as host-specificity determinants [28, 60]. Interestingly, ALPHAFOLD predicts *PWL2* to adopt a MAX effector fold [61]. In our study, however, gene knock-in experiments with *MAX79*, *MAX83*, and *MAX89* - specifically absent from the *Oryza*-infecting lineage - did not reveal a strong effect on virulence towards a large panel of rice varieties. Hence, unlike *AVR1-CO39*, these effectors are not key determinants of host-specificity. This suggests that overcoming non-host resistance is not the only and maybe not the main evolutionary scenario behind the specific loss of MAX effectors in the *Oryza*-infecting lineage. A possible alternative mechanism that can explain massive MAX effector loss during host shifts is a lack of functionality in the novel host. Some MAX effectors from a given lineage may have no function in the novel host, simply because their molecular targets are absent or too divergent in the novel host. Cellular targets of fungal effectors remain unknown for the most part, but knowledge of the molecular interactors of MAX effectors may help shed light on the drivers of their presence/absence polymorphism.

Concluding remarks

The discovery of large, structurally-similar, effector families in pathogenic fungi and the increasing availability of high-quality whole genome assemblies and high-confidence annotation tools, pave the way for in-depth investigations of the evolution of fungal effectors by

623 interdisciplinary approaches combining state-of-the-art population genomics, protein structure
624 analysis, and functional approaches. Our study on MAX effectors in the model fungus and
625 infamous cereal killer *P. oryzae* demonstrates the power of such an approach. Our investigations
626 reveal the fundamental role of directional and balancing selection in shaping the diversity of
627 MAX effector genes and pinpoint specific positions in the proteins that are targeted by these
628 evolutionary forces. This type of knowledge is still very limited on plant pathogens, and there
629 are very few studies compared to the plethoric literature on the evolution of virulence factors in
630 human pathogens. Moreover, by revealing the concerted and plastic deployment of the MAX
631 effector repertoire, our study highlights the current lack of knowledge on the regulation of these
632 processes. A major challenge will now be to identify the regulators, target proteins and mode of
633 action of MAX effectors, in order to achieve a detailed understanding of the relationships
634 between the structure, function and evolution of these proteins.

METHODS

Genome assemblies, gene prediction, and pan-genome analyses

Among the 120 genome assemblies included in our study, 66 were already publicly available, and 54 were newly assembled (S1 Table). For the 54 newly assembled genomes, reads were publicly available for 50 isolates, and four additional isolates were sequenced (available under BioProject PRJEB47684). For the four sequenced isolates, DNA was extracted using the same protocol as in ref. [62]. For the 54 newly generated assemblies, CUTADAPT [63] was used for trimming and removing low-quality reads, reads were assembled with ABYSS 2.2.3 [64] using eight different K-mer sizes, and we chose the assembly produced with the K-mer size that yielded the largest N50. For all 120 genome assemblies, genes were predicted by BRAKER 1 [65] using RNAseq data from ref. [21] and protein sequences of isolate 70-15 (Ensembl Fungi release 43). To complement predictions from BRAKER, we also predicted genes using AUGUSTUS 3.4.0 [56][3] with RNAseq data from ref. [21], protein sequences of isolate 70-15 (Ensembl Fungi release 43), and *Magnaporthe grisea* as the training set. Gene predictions from BRAKER and AUGUSTUS were merged by removing the genes predicted by AUGUSTUS that overlapped with genes predicted by BRAKER. Repeated elements were masked with REPEATMASKER 4.1.0 (<http://www.repeatmasker.org/>). The quality of genome assembly and gene prediction was checked using BUSCO [32]. The homology relationships among predicted genes were identified using ORTHOFINDER v2.4.0 [36]. The size of pan- and core-genomes was estimated using rarefaction, by resampling combinations of one to 119 genomes, taking a maximum of 100 resamples by pseudo-sample size. Sequences for each orthogroup were aligned at the codon level (i.e., keeping sequences in coding reading frame) with TRANSLATORX [66], using MAFFT v7 [67] as the aligner and default parameters for GBLOCKS [68].

Identification of effectors sensu lato, and MAX effectors

We predicted the secretome by running SIGNALP 4.1 [69], TARGET [70], and PHOBIUS [62] to identify signal peptides in the translated coding sequences of 12000 orthogroups. Only proteins

predicted to be secreted by at least two methods were retained. Transmembrane domains were identified using TMHMM [71] and proteins with a transmembrane domain outside the 30 first amino acids were excluded from the predicted secretome. Endoplasmic reticulum proteins were identified with PS-SCAN (https://ftp.expasy.org/databases/prosite/ps_scan/), and excluded.

To identify MAX effectors, we used the same approach as in the original study that described MAX effectors [17]. We first used PSI-BLAST [33] to search for homologs of known MAX effectors (AVR1-CO39, AVR-Pia, AvrPiz-t, AVR-PikD, and ToxB) in the predicted secretome. Significant PSI-BLAST hits (e-value < e-4) were aligned using a structural alignment procedure implemented in TM-ALIGN [35]. Three rounds of HMMER [34] searches were then carried out, each round consisting of alignment using TM-ALIGN, model building using HMMBUILD, and HMM search using HMMSEARCH (e-value < e-3). Only proteins with two expected, conserved Cysteines less than 33-48 amino acids apart were retained in the first two rounds of HMMER searches, as described in ref. [17].

Subsequent evolutionary analyses were conducted on three sets of orthogroups: MAX effectors, putative effectors, and other genes. The “MAX” group corresponded to 80 orthogroups for which at least 10% of sequences were identified as MAX effectors. The “secreted proteins” groups corresponded to 3283 orthogroups that were not included in the MAX group, and for which at least 10% of sequences were predicted to be secreted proteins. The last group included the remaining 11404 orthogroups.

For missing MAX effector sequences, we conducted an additional similarity search to correct for gene prediction errors. For a given MAX orthogroup and a given isolate, if a MAX effector was missing, we used BLAST-N to search for significant hits using the longest sequence of the orthogroup as the query sequence, and the isolate’s genome assembly as the subject sequence (S3 Table). We also corrected annotation errors, such as the presence of very short (typically <50bp) or very long (typically >500bp) introns, missing terminal exons associated with premature stops, or frameshifts caused by indels. All these annotation errors were checked, and corrected manually if needed, using the RNAseq data used in gene prediction in the

INTEGRATIVE GENOME VIEWER [72, 73]. We also found that some orthogroups included chimeric gene resulting from erroneous merging of two genes that were adjacent in assemblies. This was the case for orthogroups OG0000093 and OG0010985, and we used RNA-seq data in the INTEGRATIVE GENOME VIEWER to split the merged genic sequences and keep only the sequence that corresponded to a MAX effector.

For evolutionary analyses conducted on single-copy orthologs, the 11 orthogroups that included paralogous copies of MAX effectors were split into sets of orthologous sequences using genealogies inferred using RAXML v8 [37], yielding a total of 94 single-copy MAX orthologs, of which 90 orthologs passed our filters on length and sample size to be included in evolutionary analyses (see below). For each split orthogroup, sets of orthologous sequences were assigned a number that was added to the orthogroup's identifier as a suffix (for instance paralogous sequences of orthogroup OG0000244 were split into orthogroups OG0000244_1 and OG0000244_2). Sequences were re-aligned using TRANSLATORX (see above) after splitting orthogroups.

All genome assemblies, aligned coding sequences for all orthogroups and single-copy orthologs are available in Zenodo, doi: 10.5281/zenodo.7689273.

Homology modeling of MAX effectors

To check that orthogroups predicted to be MAX effectors had the typical 3D structure of MAX effectors with two beta sheets of three beta strands each, eight experimental structures with MAX-like folds were selected as 3D templates for homology modeling (PDB identifiers of the templates: 6R5J, 2MM0, 2MM2, 2MYW, 2LW6, 5A6W, 5Z1V, 5ZNG). For each of the 94 MAX orthologous groups, one representative protein was selected and homology models of this 1D query relative to each 3D template were built using MODELLER [74] with many alternative query-template threading alignments. The structural models generated using the alternative alignments were evaluated using a combination of different structural scores (DFIRE [75], GOAP [76], QMEAN [77]). Our homology modeling procedure will be described with more details in a

manuscript currently in preparation. The best structural models for the 94 representative sequences of each group of MAX orthologs are available at <https://pat.cbs.cnrs.fr/magmax/model/>. The correspondence between MAX orthogroups identifiers used in homology modeling and MAX orthogroups identifiers resulting from gene prediction is given in S2 Table.

Evolutionary analyses

Lineage-level analyses were conducted on a dataset from which divergent or introgressed isolates were removed (G17 from *Eragrostis*, Bm88324 & Bd8401 from *Setaria*, 87-120; BF0072 and BN0019 from *Oryza*; IR0088 from *Echinochloa*), to limit the impact of population subdivision within lineages. The *Stenotaphrum*-infecting lineage was not included in lineage-level analyses due to the small sample size.

Nucleotide diversity [78] and population differentiation [43] were estimated using EGGLIB v3 [79]. Sites with more than 30% missing data were excluded. Orthogroups with less than 10 sequences ($n_{eff} < 10$, n_{eff} being the average number of used samples among sites that passed the missing data filter) or shorter than 30bp ($l_{eff} < 30$, l_{eff} being the number of sites used for analysis after filtering out sites with too many missing data) were excluded from computations. For analyses of polymorphism at secondary structure annotations, the cutoff on l_{eff} was set at 10bp.

For the computation of d_N/d_S and quantification of adaptive evolution, we used isolate NI919 of *Pyricularia* sp. LS [45, 46] as the outgroup (assembly GCA_004337975.1, European Nucleotide Archive). Genes were predicted in the outgroup assembly using EXONERATE v2.2 CODING2GENOME [80]. For each gene, the query sequence was a *P. oryzae* sequence randomly selected among sequences with the fewest missing data. In parsing EXONERATE output, we

selected the sequence with the highest score, with a length greater than half the length of the query sequence.

The d_N/d_S ratio was estimated using a maximum likelihood approach (runmode=-2, CodonFreq=2 in CODEML [81]), in pairwise comparisons of protein coding sequences (*i.e.*, without using a phylogeny). For each d_N/d_S we randomly selected 12 ingroup sequences and computed the average d_N/d_S across the 12 ingroup/outgroup pairs.

Kruskal-Wallis tests were performed using the SCIPY.STATS.KRUSKAL library in PYTHON 3.7. Posthoc Mann-Whitney U-tests were performed using the SCIKIT_POSTHOC library in PYTHON 3.7, with p-values adjusted using the Bonferroni-Holm method.

Constructs for the transformation of fungal isolates

PCR products used for cloning were generated using the Phusion High-Fidelity DNA Polymerase (Thermo Fisher) and the primers listed in S7 Table. Details of the constructs are given in S8 Table. Briefly, the pSC642 plasmid (derived from the pCB1004 vector), containing a cassette for the expression of a gene of interest under the control of the *AVR-Pia* promoter (*pAVR-Pia*) and the *Neurospora crassa* β -tubulin terminator (*t-tub*), was amplified by PCR with primers oML001 and oTK609 for the insertion of MAX genes listed in S9 Table. The MAX genes *Mo_US0071_000070* (MAX79), *Mo_US0071_046730* (MAX89) and *Mo_US0071_115900* (MAX83), amplified by PCR from genomic DNA of the *P. oryzae* isolate US0071, were inserted into this vector using the Gibson Assembly Cloning Kit (New England BioLabs). The final constructs were linearized using the KpnI restriction enzyme (Promega) before *P. oryzae* transformation.

Plant and fungal growth conditions

Rice plants (*Oryza sativa*) were grown in a glasshouse in a substrate of 31% coconut peat, 30% Baltic blond peat, 15% Baltic black peat, 10% perlite, 9% volcanic sand, and 5% clay, supplemented with 3.5 g.L⁻¹ of fertilizer (Basacote® High K 6M, NPK 13-5-18). Plants were

grown under a 12h-light photoperiod with a day-time temperature of 27°C, night-time temperature of 21°C, and 70% humidity. For spore production, the wild-type and transgenic isolates of *P. oryzae* Guy11 were grown for 14 days at 25°C under a 12h-light photoperiod on rice flour agar medium (20 g.L⁻¹ rice seed flour, 2.5 g.L⁻¹ yeast extract, 1.5% agar, 500.000U penicillin g), supplemented with 240 µg.ml⁻¹ hygromycin for transgenic isolates. For mycelium production, plugs of mycelium of *P. oryzae* Guy11 were grown in liquid medium (10 g.L⁻¹ glucose, 3 g.L⁻¹ KNO₃, 2 g.L⁻¹ KH₂PO₄, 2.5 g.L⁻¹ yeast extract, 500 000U penicillin g) for 5 days at 25°C in the dark under agitation.

Fungal transformation

Protoplasts from the isolate Guy11 of *P. oryzae* were transformed by heat shock with 10µg of KpnI-linearized plasmids for the expression of MAX effectors or RFP as described previously [74]. After two rounds of antibiotic selection and isolation of monospores, transformed isolates were genotyped by Phire Plant Direct PCR (Thermo Scientific) using primers described in S7 Table. The Guy11 transgenic isolates expressing *AVR-Pia* and *AVR1-CO39* were previously generated [82, 83].

Fungal growth and infection assays

For the analysis of interaction phenotypes, leaves of three-week-old rice plants were spray-inoculated with conidial suspensions (40 000 conidia.ml⁻¹ in water with 0.5% gelatin). Plants were incubated for 16 hours in the dark at 25°C and 95% relative humidity, and then grown for six days in regular growth conditions. Seven days after inoculation, the youngest leaf that was fully expanded at the time of inoculation was collected and scanned (Scanner Epson Perfection V370) for further symptoms analyses. Phenotypes were qualitatively classified according to lesion types: no lesion or small brown spots (resistance), small lesions with a pronounced brown border and a small gray center (partial resistance), and larger lesions with a large gray center or dried leaves (susceptibility). For the analysis of gene expression, plants were spray-

inoculated with conidial suspensions at 50 000 conidia.ml⁻¹ (in water with 0.5% gelatin), and leaves were collected three days after inoculation.

RNA extraction and qRT-PCR analysis

Total RNA extraction from rice leaves or Guy11 mycelium and reverse transcription were performed as described by ref. [84]. Briefly, frozen leaves and mycelium were mechanically ground. RNA was extracted using TRI-reagent® (Sigma-Aldrich) and chloroform separation. Denaturated RNA (5µg) was retrotranscribed and used for quantitative PCR using GoTaq qPCR Master Mix according to the manufacturer's instructions (Promega) at a dilution of 1/10 for mycelium and 1/7 for rice leaves. The primers used are described in S7 Table. Amplification was performed as described by ref. [84] using a LightCycler480 instrument (Roche), and data were extracted using the instrument software. To calculate *MAX* gene expressions, the 2^{-ΔΔCT} method and primers measured efficiency were used. Gene expression levels are expressed relative to the expression of constitutive reference gene *MoEF1α*.

Statistical analyses of phenotypic data

For expression comparison between Kitaake and Maratelli infection, all analyses were performed using R (<http://www.r-project.org>). The entire kinetic experiment was repeated three times with five biological replicates for each time point. For each variety, gene, and experimental replicate, values corresponding to the day post-inoculation with the highest median expression were extracted for statistical analyses. Expression data were not normally distributed so for each gene, differences between varieties were evaluated using non-parametric Mann-Whitney U-tests.

SUPPLEMENTARY MATERIALS

S1 Table. Genomic assemblies with metadata.

S2 Table. Nomenclature of MAX effectors.

- 824 S3 Table. Presence /absence of MAX effector orthologs.
- 825 S4 Table. The expression of MAX79, MAX83 and MAX89 in Guy11 does not trigger recognition in a panel of
- 826 rice varieties.
- 827 S5 Table. Gene average of summary statistics of polymorphism, differentiation and divergence.
- 828 S6 Table. π_N and d_N/d_S in different classes of secondary structure annotations for MAX effectors with
- 829 $\pi_N/\pi_S > 1$ and $d_N/d_S > 1$, respectively.
- 830 S7 Table. Primers for cloning and expression analyses.
- 831 S8 Table. Vector constructs.
- 832 S9 Table. Sequences of the MAX effectors in the isolate US0071 that were used for the complementation of Guy11.
- 833
- 834 S1 Figure. Expression patterns of MAX effectors during rice infection.
- 835 S2 Figure. Differential expression levels of MAX effectors upon infection of two different rice cultivars.
- 836 S3 Figure. Nucleotide diversity (π), ratio of non-synonymous to synonymous nucleotide diversity (π_N/π_S),
- 837 orthogroup frequency for MAX effectors, other secreted proteins, and other genes.
- 838 S4 Figure. Assembly size, number of predicted genes, and number of orthogroups in lineages of *M. oryzae*.
- 839 S5 Figure. MAX79, MAX83 and MAX89 are expressed in the transgenic Guy11 isolates upon rice
- 840 inoculation.
- 841 S6 Figure. F_{ST} versus π_N/π_S at MAX effectors
- 842 S7 Figure. Secondary structure annotations of MAX effectors aligned with TM-ALIGN.
- 843
- 844 S1 Data. Summary statistics per orthogroup.
- 845 S2 Data. Summary statistics per MAX effector ortholog, species wide, and per lineage.
- 846

847 REFERENCES

- 848 1. Schulze-Lefert P, Panstruga R. A molecular evolutionary concept connecting nonhost resistance,
849 pathogen host range, and pathogen speciation. Trends in Plant Science. 2011;16(3):117-25. doi:
850 10.1016/j.tplants.2011.01.001.
- 851 2. Sánchez-Vallet A, Fouché S, Fudal I, Hartmann FE, Soyer JL, Tellier A, et al. The genome biology of
852 effector gene evolution in filamentous plant pathogens. Annual review of phytopathology. 2018;56:21-40.
- 853 3. Haldane JBS. Disease and evolution. Ricerca Scient 1949;19:68-76.
- 854 4. Flor HH. Inheritance of pathogenicity in *Melampsora lini*. Phytopathology. 1942;32:653-69.
- 855 5. Barrett JA. Frequency-dependent selection in plant-fungal interactions. Philosophical
856 Transactions of the Royal Society of London B, Biological Sciences. 1988;319(1196):473-83.
- 857 6. Bergelson J, Kreitman M, Stahl EA, Tian D. Evolutionary dynamics of plant R-genes. Science.
858 2001;292(5525):2281-5.
- 859 7. Brown JKM. Chance and selection in the evolution of barley mildew. Trends in Microbiology.
860 1994;2(12):470-5. PubMed PMID: 29.
- 861 8. Brown JKM. Durable resistance of crops to disease: a Darwinian perspective. Annual review of
862 phytopathology. 2015;53:513-39.
- 863 9. Stahl EA, Dwyer G, Mauricio R, Kreitman M, Bergelson J. Dynamics of disease resistance
864 polymorphism at the Rpm1 locus of Arabidopsis. Nature. 1999;400(6745):667-71.
- 865 10. Gladieux P, van Oosterhout C, Fairhead S, Jouet A, Ortiz D, Ravel S, et al. Extensive immune
866 receptor repertoire diversity in disease-resistant rice landraces. bioRxiv. 2022:2022-12.
- 867 11. Bakker EG, Toomajian C, Kreitman M, Bergelson J. A genome-wide survey of R gene
868 polymorphisms in Arabidopsis. The Plant cell. 2006;18(8):1803-18.
- 869 12. Bakker EG, Traw MB, Toomajian C, Kreitman M, Bergelson J. Low levels of polymorphism in genes
870 that control the activation of defense response in Arabidopsis thaliana. Genetics. 2008;178(4):2031-43.
- 871 13. Ebert D, Fields PD. Host-parasite co-evolution and its genomic signature. Nature Reviews
872 Genetics. 2020;21(12):754-68.
- 873 14. Ebbole DJ, Chen M, Zhong Z, Farmer N, Zheng W, Han Y, et al. Evolution and Regulation of a Large
874 Effector Family of *Pyricularia oryzae*. Molecular Plant-Microbe Interactions. 2021;34(3):255-69.
- 875 15. Seong K, Krasileva KV. Computational structural genomics unravels common folds and novel
876 families in the secretome of fungal phytopathogen *Magnaporthe oryzae*. Molecular Plant-Microbe
877 Interactions. 2021;34(11):1267-80.
- 878 16. Seong K, Krasileva KV. Prediction of effector protein structures from fungal phytopathogens
879 enables evolutionary analyses. Nature Microbiology. 2023;8(1):174-87.
- 880 17. de Guillen K, Ortiz-Vallejo D, Gracy J, Fournier E, Kroj T, Padilla A. Structure analysis uncovers a
881 highly diverse but structurally conserved effector family in phytopathogenic fungi. PLoS Pathog.
882 2015;11(10):e1005228.
- 883 18. Savary S, Willocquet L, Pethybridge SJ, Esker P, McRoberts N, Nelson A. The global burden of
884 pathogens and pests on major food crops. Nature ecology & evolution. 2019;3(3):430.
- 885 19. Fernandez J, Orth K. Rise of a cereal killer: the biology of *Magnaporthe oryzae* biotrophic growth.
886 Trends in microbiology. 2018;26(7):582-97.
- 887 20. Couch BC, Fudal I, Lebrun M-H, Tharreau D, Valent B, van Kim P, et al. Origins of Host-Specific
888 Populations of the Blast Pathogen *Magnaporthe oryzae* in Crop Domestication With Subsequent Expansion
889 of Pandemic Clones on Rice and Weeds of Rice. Genetics. 2005;170(2):613-30. PubMed PMID: 61.
- 890 21. Pordel A, Ravel S, Charriat F, Gladieux P, Cros-Arteil S, Milazzo J, et al. Tracing the origin and
891 evolutionary history of *Pyricularia oryzae* infecting maize and barnyard grass. Phytopathology.
892 2021;111(1):128-36.
- 893 22. Kato H, Yamamoto M, Yamaguchi-Ozaki T, Kadouchi H, Iwamoto Y, Nakayashiki H, et al.
894 Pathogenicity, mating ability and DNA restriction fragment length polymorphisms of *Pyricularia*
895 populations isolated from Gramineae, Bambusideae and Zingiberaceae plants. Journal of General Plant
896 Pathology. 2000;66:30-47.
- 897 23. Urashima AS, Igarashi S, Kato H. Host range, mating type, and fertility of *Pyricularia grisea* from
898 wheat in Brazil. Plant Disease. 1993;77(12):1211-6.
- 899 24. Igarashi S. *Pyricularia* em trigo. 1. Ocorrência de *Pyricularia* sp no estado do Paraná. Fitopatol
900 Bras. 1986;11:351-2.
- 901 25. Milazzo J, Pordel A, Ravel S, Tharreau D. First scientific report of *Pyricularia oryzae* causing gray
902 leaf spot disease on perennial ryegrass (*Lolium perenne*) in France. Plant Disease. 2019;103(5):1024-.

26. Islam MT, Croll D, Gladieux P, Soanes DM, Persoons A, Bhattacharjee P, et al. Emergence of wheat blast in Bangladesh was caused by a South American lineage of *Magnaporthe oryzae*. *BMC biology*. 2016;14(1):84.
27. Gladieux P, Condon B, Ravel S, Soanes D, Maciel JLN, Nhani A, et al. Gene Flow between Divergent Cereal- and Grass-Specific Lineages of the Rice Blast Fungus *Magnaporthe oryzae*. *mBio*. 2018;9(1).
28. Sweigard JA, Carroll AM, Kang S, Farrall L, Chumley FG, Valent B. Identification, Cloning, and Characterization of *PWL2*, a Gene for Host Species Specificity in the Rice Blast Fungus. *The Plant cell*. 1995;7(8):1221-33. PubMed PMID: 260.
29. Inoue Y, Vy TTP, Yoshida K, Asano H, Mitsuoka C, Asuke S, et al. Evolution of the wheat blast fungus through functional losses in a host specificity determinant. *Science*. 2017;357(6346):80-3.
30. Asuke S, Tanaka M, Hyon G-S, Inoue Y, Vy TTP, Niwamoto D, et al. Evolution of an Eleusine-specific subgroup of *Pyricularia oryzae* through a gain of an avirulence gene. *Molecular Plant-Microbe Interactions*. 2020;33(2):153-65.
31. Zheng Y, Zheng W, Lin F, Zhang Y, Yi Y, Wang B, et al. AVR1-CO39 is a predominant locus governing the broad avirulence of *Magnaporthe oryzae* 2539 on cultivated rice (*Oryza sativa* L.). *Molecular plant-microbe interactions*. 2011;24(1):13-7.
32. Simão FA, Waterhouse RM, Ioannidis P, Kriventseva EV, Zdobnov EM. BUSCO: assessing genome assembly and annotation completeness with single-copy orthologs. *Bioinformatics*. 2015;31(19):3210-2.
33. Altschul SF, Madden TL, Schäffer AA, Zhang J, Zhang Z, Miller W, et al. Gapped BLAST and PSI-BLAST: a new generation of protein database search programs. *Nucleic acids research*. 1997;25(17):3389-402.
34. Finn RD, Clements J, Eddy SR. HMMER web server: interactive sequence similarity searching. *Nucleic acids research*. 2011;39(suppl_2):29-37.
35. Zhang Y, Skolnick J. TM-align: a protein structure alignment algorithm based on the TM-score. *Nucleic acids research*. 2005;33(7):2302-9.
36. Emms DM, Kelly S. OrthoFinder: solving fundamental biases in whole genome comparisons dramatically improves orthogroup inference accuracy. *Genome biology*. 2015;16(1):157.
37. Stamatakis A. RAxML version 8: a tool for phylogenetic analysis and post-analysis of large phylogenies. *Bioinformatics*. 2014;30(9):1312-3.
38. Frichot E, Mathieu F, Trouillon T, Bouchard G, François O. Fast and efficient estimation of individual ancestry coefficients. *Genetics*. 2014;196(4):973-83.
39. Huson DH, Bryant D. Application of Phylogenetic Networks in Evolutionary Studies. *Molecular Biology and Evolution*. 2006;23(2):254-67.
40. Tosa Y, Osue J, Eto Y, Oh H-S, Nakayashiki H, Mayama S, et al. Evolution of an avirulence gene, AVR1-CO39, concomitant with the evolution and differentiation of *Magnaporthe oryzae*. *Molecular Plant-Microbe Interactions*. 2005;18(11):1148-60.
41. Cesari S, Thilliez G, Ribot C, Chalvon V, Michel C, Jauneau A, et al. The rice resistance protein pair RGA4/RGA5 recognizes the *Magnaporthe oryzae* effectors AVR-Pia and AVR1-CO39 by direct binding. *The Plant cell*. 2013;25(4):1463-81. Epub 2013/04/04. doi: 10.1105/tpc.112.107201. PubMed PMID: 23548743; PubMed Central PMCID: PMC3663280.
42. Okuyama Y, Kanzaki H, Abe A, Yoshida K, Tamiru M, Saitoh H, et al. A multifaceted genomics approach allows the isolation of the rice Pia-blast resistance gene consisting of two adjacent NBS-LRR protein genes. *The Plant Journal*. 2011;66(3):467-79.
43. Weir BS, Cockerham CC. Estimating F-statistics for the analysis of population structure. *Evolution*. 1984;38:1358-70. PubMed PMID: 283.
44. Hahn MW. *Molecular population genetics*: Oxford University Press; 2018.
45. Hirata K, Kusaba M, Chuma I, Osue J, Nakayashiki H, Mayama S, et al. Speciation in *Pyricularia* inferred from multilocus phylogenetic analysis. *Mycological Research*. 2007;111(7):799-808.
46. Gómez Luciano LB, Tsai IJ, Chuma I, Tosa Y, Chen Y-H, Li J-Y, et al. Blast fungal genomes show frequent chromosomal changes, gene gains and losses, and effector gene turnover. *Molecular Biology and Evolution*. 2019;36(6):1148-61.
47. Yang Z. Likelihood ratio tests for detecting positive selection and application to primate lysozyme evolution. *Molecular biology and evolution*. 1998;15(5):568-73.
48. Frishman D, Argos P. Knowledge-based protein secondary structure assignment. *Proteins: Structure, Function, and Bioinformatics*. 1995;23(4):566-79.
49. Clay K, Kover PX. The Red Queen hypothesis and plant/pathogen interactions. *Annual review of Phytopathology*. 1996;34(1):29-50.
50. Van Valen L. A new evolutionary law. 1973.

- 961 51. Yang Z, Bielawski JP. Statistical methods for detecting molecular adaptation. Trends in ecology &
962 evolution. 2000;15(12):496-503.
- 963 52. Yan X, Tang B, Ryder LS, MacLean D, Were VM, Eseola AB, et al. The transcriptional landscape of
964 plant infection by the rice blast fungus *Magnaporthe oryzae* reveals distinct families of temporally co-
965 regulated and structurally conserved effectors. bioRxiv. 2022:2022-07.
- 966 53. Chiapello H, Mallet L, Guerin C, Aguilera G, Amselem J, Kroj T, et al. Deciphering Genome Content
967 and Evolutionary Relationships of Isolates from the Fungus *Magnaporthe oryzae* Attacking Different Host
968 Plants. Genome Biol Evol. 2015;7(10):2896-912. Epub 2015/10/11. doi: 10.1093/gbe/evv187. PubMed
969 PMID: 26454013; PubMed Central PMCID: PMC4684704.
- 970 54. Soyer JL, El Ghalid M, Glaser N, Ollivier B, Linglin J, Grandaubert J, et al. Epigenetic control of
971 effector gene expression in the plant pathogenic fungus *Leptosphaeria maculans*. PLoS genetics.
972 2014;10(3):e1004227.
- 973 55. Tang B, Yan X, Ryder LS, Cruz-Mireles N, Soanes DM, Molinari C, et al. Rgs1 is a regulator of
974 effector gene expression during plant infection by the rice blast fungus *Magnaporthe oryzae*. bioRxiv.
975 2022:2022-09.
- 976 56. Fall LA, Salazar MM, Drnevich J, Holmes JR, Tseng M-C, Kolb FL, et al. Field pathogenomics of
977 *Fusarium* head blight reveals pathogen transcriptome differences due to host resistance. Mycologia.
978 2019;111(4):563-73.
- 979 57. Sonah H, Zhang X, Deshmukh RK, Borhan MH, Fernando WGD, Belanger RR. Comparative
980 transcriptomic analysis of virulence factors in *Leptosphaeria maculans* during compatible and
981 incompatible interactions with canola. Frontiers in plant science. 2016;7:1784.
- 982 58. Arora S, Steed A, Goddard R, Gaurav K, O'Hara T, Schoen A, et al. A wheat kinase and immune
983 receptor form host-specificity barriers against the blast fungus. Nature Plants. 2023:1-8.
- 984 59. Farman ML, Eto Y, Nakao T, Tosa Y, Nakayashiki H, Mayama S, et al. Analysis of the structure of the
985 *AVR1-Co39* avirulence locus in virulent rice-infecting isolates of *Magnaporthe grisea*. Molecular Plant-
986 Microbe Interactions. 2002;15:6-16. PubMed PMID: 90.
- 987 60. Kang S, Sweigard JA, Valent B, Valent B. The PWL host specificity gene family in the blast
988 fungus *Magnaporthe grisea*. Molecular Plant Microbe Interactions. 1995;(0894-0282 (Print)).
- 989 61. Brabham HJ, Gómez De La Cruz D, Were V, Shimizu M, Saitoh H, Hernández-Pinzón I, et al. Barley
990 MLA3 recognizes the host-specificity determinant PWL2 from rice blast (*M. oryzae*). bioRxiv. 2022:2022-
991 10.
- 992 62. Thierry M, Charriat F, Milazzo J, Adreit H, Ravel S, Cros-Arteil S, et al. Maintenance of divergent
993 lineages of the Rice Blast Fungus *Pyricularia oryzae* through niche separation, loss of sex and post-mating
994 genetic incompatibilities. PLoS pathogens. 2022;18(7):e1010687.
- 995 63. Martin M. Cutadapt removes adapter sequences from high-throughput sequencing reads. EMBnet
996 journal. 2011;17(1):10-2.
- 997 64. Simpson JT, Wong K, Jackman SD, Schein JE, Jones SJM, Birol I. ABySS: a parallel assembler for
998 short read sequence data. Genome research. 2009;19(6):1117-23.
- 999 65. Hoff KJ, Lange S, Lomsadze A, Borodovsky M, Stanke M. BRAKER1: unsupervised RNA-Seq-based
1000 genome annotation with GeneMark-ET and AUGUSTUS. Bioinformatics. 2015;32(5):767-9.
- 1001 66. Abascal F, Zardoya R, Telford MJ. TranslatorX: multiple alignment of nucleotide sequences guided
1002 by amino acid translations. Nucleic acids research. 2010;38(suppl_2):W7-W13.
- 1003 67. Katoh K, Toh H. Recent developments in the MAFFT multiple sequence alignment program.
1004 Briefings in Bioinformatics. 2008;9(4):286-98. doi: 10.1093/bib/bbn013. PubMed PMID:
1005 ISI:000256756400004.
- 1006 68. Castresana J. Selection of conserved blocks from multiple alignments for their use in phylogenetic
1007 analysis. Molecular biology and evolution. 2000;17(4):540-52.
- 1008 69. Petersen TN, Brunak S, Von Heijne G, Nielsen H. SignalP 4.0: discriminating signal peptides from
1009 transmembrane regions. Nature methods. 2011;8(10):785-6.
- 1010 70. Emanuelsson O, Nielsen H, Brunak S, Von Heijne G. Predicting subcellular localization of proteins
1011 based on their N-terminal amino acid sequence. Journal of molecular biology. 2000;300(4):1005-16.
- 1012 71. Krogh A, Larsson B, Von Heijne G, Sonnhammer ELL. Predicting transmembrane protein topology
1013 with a hidden Markov model: application to complete genomes. Journal of molecular biology.
1014 2001;305(3):567-80.
- 1015 72. Robinson JT, Thorvaldsdóttir H, Turner D, Mesirov JP. igv.js: an embeddable JavaScript
1016 implementation of the Integrative Genomics Viewer (IGV). Bioinformatics. 2023;39(1):btac830.
- 1017 73. Robinson JT, Thorvaldsdóttir H, Winckler W, Guttman M, Lander ES, Getz G, et al. Integrative
1018 genomics viewer. Nature biotechnology. 2011;29(1):24-6.

1019 74. Webb B, Sali A. Protein Structure Modeling with MODELLER. *Methods Mol Biol.* 2021;2199(1940-
1020 6029 (Electronic)):239–55.

1021 75. Zhou H, Zhou Y. Distance-scaled, finite ideal-gas reference state improves structure-derived
1022 potentials of mean force for structure selection and stability prediction. *Protein science.*
1023 2002;11(11):2714-26.

1024 76. Zhou H, Skolnick J. GOAP: a generalized orientation-dependent, all-atom statistical potential for
1025 protein structure prediction. *Biophysical journal.* 2011;101(8):2043-52.

1026 77. Benkert P, Tosatto SCE, Schomburg D. QMEAN: A comprehensive scoring function for model
1027 quality assessment. *Proteins: Structure, Function, and Bioinformatics.* 2008;71(1):261-77.

1028 78. Tajima F. Evolutionary relationship of DNA sequences in finite populations. *Genetics.*
1029 1983;105(2):437-60.

1030 79. Siol M, Coudoux T, Ravel S, De Mita S. EggLib 3: A python package for population genetics and
1031 genomics. *Molecular Ecology Resources.* 2022;22(8):3176-87.

1032 80. Slater GSC, Birney E. Automated generation of heuristics for biological sequence comparison. *BMC*
1033 *bioinformatics.* 2005;6(1):1-11.

1034 81. Yang Z. PAML: a program package for phylogenetic analysis by maximum likelihood. *Computer*
1035 *applications in the biosciences.* 1997;13(5):555-6.

1036 82. Ribot C, Césari S, Abidi I, Chalvon V, Bournaud C, Vallet J, et al. The *Magnaporthe oryzae* effector
1037 AVR 1-CO 39 is translocated into rice cells independently of a fungal-derived machinery. *The Plant*
1038 *Journal.* 2013;74(1):1-12.

1039 83. Ortiz D, De Guillen K, Cesari S, Chalvon V, Gracy J, Padilla A, et al. Recognition of the *Magnaporthe*
1040 *oryzae* effector AVR-Pia by the decoy domain of the rice NLR immune receptor RGA5. *The Plant cell.*
1041 2017;29(1):156-68.

1042 84. Pélissier R, Buendia L, Brousse A, Temple C, Ballini E, Fort F, et al. Plant neighbour-modulated
1043 susceptibility to pathogens in intraspecific mixtures. *Journal of experimental botany.* 2021;72(18):6570-
1044 80.

1045